

# PARAMETRIC ANALYSIS OF THE EFFICIENCY OF THE COMBINED GAS-STEAM TURBINE UNIT OF A HYBRID CYCLE FOR THE FPSO VESSEL

Serhiy Serbin\*<sup>1</sup>

Nikolay Washchilenko<sup>1</sup>

Marek Dzida<sup>2</sup>

Jerzy Kowalski<sup>2</sup>

<sup>1</sup> Admiral Makarov National University of Shipbuilding, Ukraine

<sup>2</sup> Gdańsk University of Technology, Poland

\* Corresponding author: [serbin1958@gmail.com](mailto:serbin1958@gmail.com) (S. Serbin)

## ABSTRACT

*A thermal diagram of the combined gas-steam turbine unit of a hybrid cycle, which is an energy complex consisting of a base gas turbine engine with a steam turbine heat recovery circuit and a steam-injected gas turbine operating with overexpansion, is proposed. A mathematical model of a power plant has been developed, taking into consideration the features of thermodynamic processes of simple, binary, and steam-injected gas-steam cycles. Thermodynamic investigations and optimization of the parameters of a combined installation of a hybrid cycle for the generation of electrical energy have been carried out. Three-dimensional calculations of the combustion chamber of a steam-injected gas turbine were carried out, which confirmed the low emissions of the main toxic components.*

**Keywords:** Combined-cycle, Gas turbine, Steam turbine, Power plant

## SYMBOLS AND ABBREVIATIONS

$C$	Molar concentration, mol/m <sup>3</sup>	$v$	Velocity, m/s
$C_N$	Specific fuel consumption, kg/(kW·h)	$X$	Mass fraction; relative steam flow rate
$c_p$	Average mass heat capacity, kJ/(kg·K)	$x$	Dryness factor
$D$	Diffusion coefficient, m <sup>2</sup> /s	$Y$	Mass concentration, kg/m <sup>3</sup>
$d$	Relative steam content	$\alpha$	Air excess coefficient; discharge coefficient
$E$	Activation energy, J/mol	$\beta$	Coefficient of leakage
$G$	Mass flow rate, kg/s	$\varepsilon$	Turbulent dissipation rate, m <sup>2</sup> /s <sup>3</sup>
$g$	Relative capacity	$\eta$	Efficiency
$H_U$	Lower calorific value of the fuel	$\pi_c$	Total pressure ratio of the compressor
$h$	Enthalpy, kJ/kg	$\rho$	Mass density, kg/m <sup>3</sup>
$k$	Circulation ratio; isentropic index; turbulent kinetic energy, m <sup>2</sup> /s <sup>2</sup>	$\nu$	Total pressure recovery coefficient
$L_0$	Stoichiometric amount of air, kg/kg	$C$	Compressor
$M$	Molecular weight, kg/mol	$CC$	Combustion chamber
$N$	Power, kW	$CDT$	Compressor drive turbine
$N_c$	Specific power, kJ/kg	$CGSTU$	Combined gas-steam turbine unit
$P$	Pressure, Pa	$GSC$	Gas-steam condenser
$R$	Gas constant, kJ/(kmol·K); rate of component's formation, mol/(m <sup>3</sup> ·s)	$GT$	Generator turbine
$T$	Temperature, K	$FPSO$	Floating Production, Storage, and Offloading vessel
		$GTA$	Gas turbine aggregate
		$GTE$	Gas turbine engine
		$HPC$	High-pressure compressor

<i>HPT</i>	High-pressure turbine
<i>HRC</i>	Heat recovery circuit
<i>HRS</i>	Heat-recovery steam generator
<i>LPC</i>	Low-pressure compressor
<i>LPT</i>	Low-pressure turbine

<i>SIGT</i>	Steam-injected gas turbine
<i>SIGTA</i>	Steam-injected gas turbine aggregate
<i>SC</i>	Steam condenser
<i>ST</i>	Steam turbine

## INTRODUCTION

Combined gas-steam turbine plants are increasingly used for the generation of electrical energy [1]. A large number of thermal circuits have been developed that allow the heat of exhaust gases from gas turbine engines (GTE) of a simple cycle in a heat recovery circuit (HRC) to be utilized for generating steam of various parameters [2-4]. Superheated steam is usually supplied to a steam turbine (ST) to generate additional power and implement a binary steam-gas cycle, or is injected into the combustion chamber (CC) of the so-called steam-injected gas turbine (SIGT) to implement a steam-injected cycle [5-6]. In the turbines of the SIGT, the expansion of the gas-steam mixture is carried out with an additional (in comparison with the GTE of a simple thermal scheme) generation of mechanical energy. To trap the moisture contained in the gas-steam mixture, it is possible to use the so-called gas-steam condenser operating at atmospheric pressure, where a large amount of water introduced into the cycle condenses, and dehydrated combustion products are released into the atmosphere. With the help of the feed pump, the water is again directed to the heat-recovery steam generator (HRS). The thermal circuit that implements such a steam-injected cycle with moisture trapping is called "Aquarius" [7]. Implementation of the SIGT cycle with steam injection into the combustion chamber makes it possible to increase the efficiency of the cycle by 22.5-30.7%, and the specific power by 49-73% in comparison with the GTE of a simple scheme [8].

Note that the combined gas-steam turbine plants are most in demand for thermal power stations, where the power capacities are very significant. Currently, the capabilities of such installations are expanding and are promising for marine applications, especially for Floating Production, Storage, and Offloading (FPSO) vessels. Power plants for the FPSO vessels are characterized by high values of the generated power, because they are designed to generate electricity for the needs of oil production, storage, and unloading of oil as well as to supply energy to various auxiliary equipment for processing crude oil and associated gas [9-10].

Many FPSO vessels are equipped with gas turbines and combined power plants. Examples are the vessels Global Producer III, Armada Olombendo, Dhirubhai-1, Pioneiro de Libra, Cidade de Itajaí, Triton, Cidade de Maricá, and others [9, 11, 12]. The total capacity of power plants is largely determined by the purpose of the vessel and varies from 30 to 150 MW, and the energy consumption is extremely irregular and is determined by the characteristics of the oil field, the production platform, and the completeness of the equipment used. In most cases, it is envisaged to use from 2 to 4 gas turbine engines, often operating at partial loads.

This investigation examines the thermal diagram of a power plant that combines the advantages of a gas turbine aggregate (GTA) with a heat recovery circuit (GTA with HRC) with the advantages of a steam-injected gas turbine aggregate (SIGTA) operating with overexpansion.

## 1. THERMAL DIAGRAM OF THE INSTALLATION

A thermal diagram of the combined gas-steam turbine unit of a hybrid cycle (CGSTU) created based on a serial gas turbine engine, which also includes a steam-injected gas turbine operating with overexpansion and a steam turbine heat recovery circuit for a serial gas turbine engine, is proposed. The GTA with HRC is designed based on the UGT25000 gas turbine engine serially produced by Zorya-Mashproekt, with a capacity of 26,700 kW and efficiency of 36.3% at ISO conditions [13]. The diagram of the proposed hybrid cycle power plant is shown in Fig. 1.

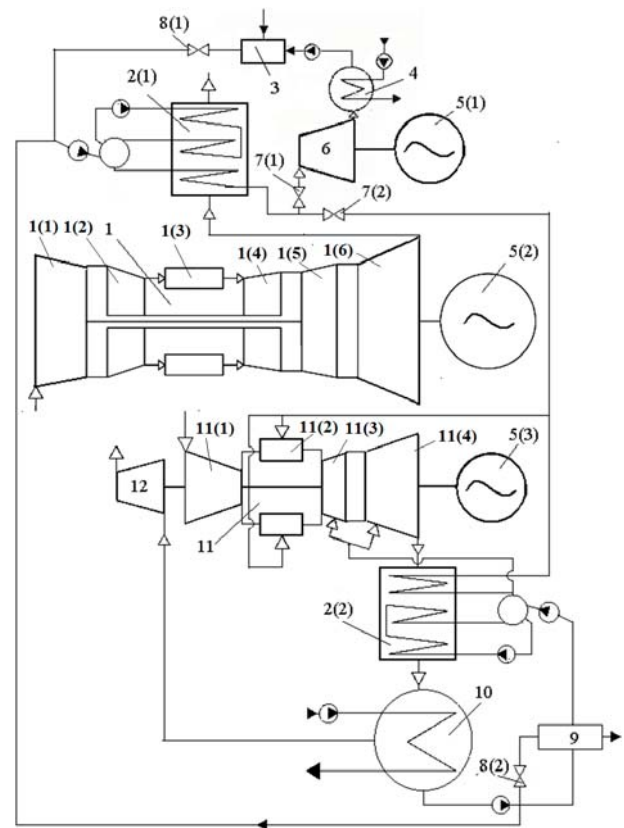


Fig. 1. Thermal diagram of the combined gas-steam turbine unit of a hybrid cycle: 1 - GTE UGT25000; 1(1) - LPC; 1(2) - HPC; 1(3) - CC; 1(4) - HPT; 1(5) - LPT; 1(6) - GT; 2(1), 2(2) - HRS; 3 - boiler water tank; 4 - steam condenser; 5(1), 5(2), 5(3) - electric generators; 6 - ST; 7(1), 7(2) - steam valves; 8(1), 8(2) - water valves; 9 - water treatment unit; 10 - gas-steam condenser; 11 - SIGT; 11(1) - C; 11(2) - CC; 11(3) - CDT; 11(4) - GT; 12 - exhauster.

The thermal diagram includes (a) a serial GTE UGT25000 '1' operating on an electric generator '5(2)', (b) a steam turbine HRC consisting of a heat recovery steam generator '2(1)' and a steam turbine '6' with the appropriate equipment, which is loaded on the electric generator '5(1)', as well as (c) a SIGTA, which includes the SIGT '11', HRSG '2(2)', as well as a gas-steam condenser '10'. The GTE '1' is developed according to the kinematic scheme with a two-spool compressor: '1(1)' - LPC and '1(2)' - HPC and involves a combustion chamber '1(3)' and three turbines: '1(4)' - HPT, '1(5)' - LPT, '1(6)' - GT. The SIGT '11' consists of a single-spool compressor '11(1)', a combustion chamber with power steam injection '11(2)', a compressor drive turbine '11(3)' and a generator turbine '11(4)'. The SIGT operates with overexpansion, which is provided by the exhauster '12', and transfers power to the electric generator '5(3)'.

The exhaust gases after the base GTE UGT25000 enter the HRC '2(1)', which generates superheated steam. The steam supply to the ST '6' and the combustion chamber of the SIGT is regulated depending on the position of the valves '7(1)' and '7(2)'. When the valve '7(1)' is open and the valve '7(2)' is closed, the CGSTU operates as a gas turbine aggregate with the single pressure steam-water HRC, and the rest of the equipment may not be used. When the valve '7(2)' is open, one part of the steam from the HRSG '2(1)' (up to 50% of its steam capacity) is injected into the CC of the SIGT '11', and the other part of the steam continues to flow to the ST '6' of the HRC of the basic gas turbine engine '1'.

The HRSG '2(2)', which is located at the exit from SIGT '11', generates superheated steam at the same pressure as the HRSG '2(1)'. Both superheated steam, which is injected to the mixing zone of the combustion chamber's flame tubes, and dry saturated steam, which is fed to the cooling of the CTD '11(3)' and GT '11(4)' nozzle and rotor blades, and also the casing of the SIGT '11', are generated.

The waste gas-steam mixture after the SIGT '11' passes through the HRSG '2(2)' and enters the gas-steam condenser '10', in which most of the steam injected into the CC, as well as steam from the cooling system of the high-temperature turbine part of the engine, is condensed into the water and, using a pump, enters the water treatment unit '9'.

After the gas-steam condenser '10', the combustion products containing the residual amount of steam enter the exhauster '12', in which they are compressed to atmospheric pressure and discharged into the atmosphere. From the water treatment unit '9', using feed pumps, water flows back to the HRSG '2(1)' and '2(2)' separators.

A thermodynamic investigation and optimization of the cycle parameters for the considered scheme of the combined CGSTU of a hybrid cycle for a thermal power station were carried out for the case of using GTE UGT25000 as a base one. The results of the efficiency of the thermal scheme were obtained taking into consideration the international standards ISO 9001-2008 (without taking into account the total pressure loss at the inlet and outlet of the engine and an ambient temperature of 288 K). In the investigation, the values of total pressure losses along the CGSTU path, the

efficiency of the turbine and compressor stages, and other similar parameters were taken under the manufacturer's recommendations [14].

It is assumed that the basic GTE will be used without changes in design and parameters. In addition to the basic gas turbine engine, a steam turbine HRC with the single pressure HRSG and optimal steam parameters, the SIGT, the HRSG '2(2)', the exhauster, and the gas-steam condenser were designed. In the proposed article, the parameters of the SIGT with HRC and overexpansion are investigated in the most detail. Note that, in this case, a significant part of the steam generated by the HRSG of the base GTE is additionally supplied to the SIGT.

## 2. MATHEMATICAL MODEL OF PROCESSES IN THE COMBINED GAS-STEAM TURBINE UNIT OF A HYBRID CYCLE

The developed mathematical model of the combined gas-steam turbine unit of a hybrid cycle for a thermal power station consists of several modules.

**Module one** is a mathematical model of a basic GTE loaded on an electric generator, which is verified according to the data of the manufacturer under ISO conditions, which are open access. This, using the method of balancing the object's thermodynamic parameters, makes it possible to obtain reliable values of some key functional parameters of the mathematical model that determine the level of technology of the produced turbomachines, as well as to estimate the values of the coefficients and parameters that are absent in the advertising materials of the manufacturer but are necessary for further calculations.

**Module two** recalculates the main parameters of the basic gas turbine engine for the conditions of its operation as part of a thermal circuit with a gas outlet pipe and a connected heat recovery steam generator HRSG '2(1)'. The coefficients of the influence of total pressure losses of the above-mentioned devices located in the exhaust duct of the gas turbine engine, obtained in the previous stage by the method of two-sided variation, are used to define the efficiency of the gas turbine engine  $\eta_g$ , the effective power of the gas turbine engine  $N_{eGTE}$ , and the temperature of the engine exhaust gases  $T_4$ .

**Module three** is a mathematical model of a steam turbine heat recovery circuit consisting of the HRSG '2(1)', a steam turbine loaded on an electric generator, a steam condenser (SC), and pumps serving the HRC equipment. It is assumed that the ST is designed to operate with the full amount of steam that the HRSG '2(1)' is capable of generating at the full power mode of the base GTE.

The steam pressure in the separator of the HRSG '2(1)' is determined by the formula

$$P_{HRSG} = \frac{P_{out} \cdot \pi_{cSIGT} \cdot v_{cc}}{v_{s3} \cdot v_{ss1} \cdot v_{id}} \quad (1)$$

where  $P_{out}$  is the outside air pressure,  $\pi_{cSIGT}$  is the total pressure ratio of the SIGT compressor,  $v_{cc}$ ,  $v_{s3}$ ,  $v_{ss1}$ ,  $v_{id}$  are the

total pressure recovery coefficients for the SIGT's combustion chamber, the steam line from the HRSG '2(1)' to the CC, the HRSG '2(1)' steam superheater, and the steam injection device, respectively.

The superheating temperature in the '2(1)' is taken according to the coupled steam parameters [10]

$$T_{ss1} = F(P_{HRSG}, \eta_{st}, x_{min}, P_Z) \quad (2)$$

where  $P_Z$  is the steam pressure in the SC,  $\eta_{st}$  is the internal efficiency of the ST, and  $x_{min}$  is the permissible rate of the steam dryness fraction after the last stage of the ST.

The relative steam capacity of the HRSG '2(1)' for superheated steam

$$g_{ss} = \frac{\beta_{l1} \cdot \beta_{go1} \cdot c_{pg4} \cdot (T_4 - T_{eb1})}{(h_{ss1} - h_{ws}) + k_c \cdot (h_{ws} - h_{w2e})} \quad (3)$$

where  $\beta_{l1}$  is the coefficient of leakage of the HRSG '2(1)',  $\beta_{go1}$  is the discharge coefficient of the base GTE's gas outlet device,  $k_c$  is the circulation ratio of the HRSG '2(1)' pump,  $c_{pg4}$  is the average mass heat capacity of the gas in the superheating and evaporating banks of the HRSG '2(1)',  $h_{ss1}$  is the enthalpy of superheated steam at the outlet of the HRSG '2(1)',  $h_{ws}$ ,  $h_{w2e}$  are the enthalpy of water at the pressure saturation line in the separator and at the outlet of the economizer bank of the HRSG '2(1)', respectively, and  $T_{eb1}$  is the temperature behind the evaporating bank.

This module also determines the power of the steam turbine, the energy consumption for the operation of the auxiliary equipment of the HRC, the power and efficiency of a thermal power station in the configuration of a combined GTA with a steam HRC.

**Module four** is a mathematical model of a steam-injected gas turbine aggregate, consisting of a SIGT operating with overexpansion and loaded onto a separate electric generator, a heat recovery steam generator HRSG '2(2)' and a gas-steam condenser (GSC). Superheated steam is supplied to the SIGT's CC both from its own HRSG '2(2)' and from the HRSG '2(1)' in the fraction  $X$  of its total steam capacity.

The relative amount of steam from the HRSG '2(1)' injected into the CC, which is necessary to achieve the specified temperature at the turbine inlet and the specified air excess coefficient  $\alpha$  in this CC, is determined by the formula

$$g_{ss1} = \frac{1}{\alpha \cdot L_0} \frac{A - B}{(h_{3s} - h_{ss}) / \alpha_{cc}} - g_{ss2} \frac{(h_{3s} - h_{ss2})}{(h_{3s} - h_{ss})} \quad (4)$$

where

$$A = H_U \cdot \eta_{cc} - [c_{p_{scp}}|_{293}^{T_3} \cdot (L_0 + 1) - c_{pa}|_{293}^{T_3} \cdot L_0] \cdot (T_3 - 293),$$

$$B = c_{pa}|_{293}^{T_3} \cdot (T_3 - 293) - c_{pa}|_{293}^{T_2} \cdot (T_2 - 293).$$

In formula (4)  $T_2$  is the air temperature behind the SIGT's compressor,  $T_3$  is the temperature of the gas-steam mixture before the SIGT's compressor turbine,  $h_{ss}$  is the enthalpy of superheated steam at the outlet from the HRSG '2(1)',  $h_{ss2}$  is the enthalpy of superheated steam at the outlet from the HRSG '2(2)',  $h_{3s}$  is the enthalpy of superheated steam in the gas-steam mixture at the outlet of the SIGT's CC,  $g_{ss2}$  is the relative steam capacity of the HRSG '2(2)' for superheated steam,  $H_U$  is the lower calorific value of the fuel,  $L_0$  is the stoichiometric amount of air,  $\alpha$  is the given value of the air excess coefficient of the SIGT's CC,  $\alpha_{cc}$  is discharge coefficient of the CC,  $\eta_{cc}$  is the coefficient of combustion completeness in the CC,  $c_{p_{scp}}$  is the average mass heat capacity of stoichiometric combustion products, and  $c_{pa}$  is the average mass heat capacity of air.

The relative steam capacity of the HRSG '2(1)' for superheated steam

$$A = H_U \cdot \eta_{cc} - [c_{p_{scp}}|_{293}^{T_3} \cdot (L_0 + 1) - c_{pa}|_{293}^{T_3} \cdot L_0] \cdot (T_3 - 293), \quad (5)$$

$$B = c_{pa}|_{293}^{T_3} \cdot (T_3 - 293) - c_{pa}|_{293}^{T_2} \cdot (T_2 - 293).$$

where  $\beta_{go2}$  is the discharge coefficient of the SIGT's gas outlet device,  $\beta_{l2}$  is the coefficient of leakage of the HRSG '2(2)',  $\Sigma g_{scoi}$  is the total relative flow rate of dry saturated steam used to cool the SIGT's turbine stages,  $c_{p_{gs4}}$  is the average mass heat capacity of the gas-steam mixture in the superheating and evaporating banks of the HRSG '2(2)',  $h_{ss2}$  is the enthalpy of superheated steam at the HRSG '2(2)' outlet,  $h_{11}$  is the enthalpy of dry saturated steam at the HRSG '2(2)' outlet,  $h_{ws2}$  is the enthalpy of water at the pressure saturation line in the separator of the HRSG '2(2)',  $T_{dgs}$  is the temperature of the gas-steam mixture at the outlet from the SIGT, and  $T_{eb2}$  is the temperature of the gas-steam mixture behind the evaporating bank of the HRSG '2(2)'.

The absolute value of the air flow rate through the SIGT's compressor is found by the formula

$$G_{cSIGT} = G_{c1} \cdot \frac{g_{ss} \cdot X}{g_{ss1}} \quad (6)$$

where  $G_{c1}$  is the air flow rate through the compressor of the base GTE.

The amount of water lost in the SIGT cycle with exhaust gases after the GSC is determined by the formula

$$G_{weg} = \frac{d_{GSC} \cdot (G_{cSIGT} \cdot \beta_{go2} - G_{w\Sigma})}{(1 - d_{GSC})} \quad (7)$$

where  $G_{w\Sigma}$  is the total amount of water vapor in the gas-steam flow before the GSC.

In formula (7), the value of the relative steam content in the flow behind the GSC,

$$d_{GSC} = \frac{R_g}{R_s \cdot \left( \frac{P_{out}}{v_{go} \cdot \pi_{ex} \cdot P_{s2}} - 1 \right) + R_g} \quad (8)$$

where  $P_{s2}$  is the partial steam pressure in the mixture behind the GSC,  $R_g$  and  $R_s$  are the gas constants for combustion products and steam, respectively,  $\pi_{ex}$  is the exhauster compression ratio, and  $\nu_{go}$  is the total pressure recovery coefficient for the exhaust SIGT's path after the exhauster.

The exhauster drive power

$$N_{ex} = (G_{cSIGT} \cdot \beta_{go_2} - G_{w\Sigma} + G_{weg}) \cdot c_{p_{ex}} \cdot \frac{T_8 \cdot (\pi_{ex}^{k_{ex}-1} - 1)}{\eta_{ex}} \quad (9)$$

where  $T_8$  is the temperature of the gas-steam mixture at the outlet of the GSC,  $c_{p_{ex}}$  is the average mass heat capacity of the gas-steam mixture in the exhauster,  $k_{ex}$  is the isentropic index for the pressure increasing process in the exhauster,  $\eta_{ex}$  is the internal adiabatic efficiency of the exhauster, and  $G_{w\Sigma}$  is the total amount of water vapor in the gas-steam flow before the GSC.

The SIGT's compressor drive power

$$N_{cSIGT} = G_{cSIGT} \cdot c_{pc} \cdot \frac{T_{ou} \cdot (\pi_{cSIGT}^{k_c-1} - 1)}{\eta_{cSIGT}} \quad (10)$$

where  $c_{pc}$  is the average mass heat capacity of air in the SIGT's compressor,  $k_c$  is the isentropic index for the pressure increasing process in the SIGT's compressor, and  $\eta_{cSIGT}$  is the internal adiabatic efficiency of the SIGT's compressor.

The effective power of the SIGT

$$N_{eSIGT} = G_{cSIGT} \cdot N_{sp_t} \cdot \eta_t - N_{cSIGT} - N_{ex} \quad (11)$$

where  $N_{sp}$  is the specific power of the SIGT's turbine part, and  $\eta_t$  is the mechanical efficiency of the SIGT's turbine part.

The total electrical power of the power plant

$$N_{eL_{CGSTU}} = N_{eSIGT} \cdot \eta_{eg_3} + N_{eGTE} \cdot \eta_{eg_2} + N_{eST} \cdot \eta_{eg_1} \quad (12)$$

where  $N_{eGTE}$  is the effective power of the base GTE,  $N_{eST}$  is the effective steam turbine power,  $\eta_{eg_1}$ ,  $\eta_{eg_2}$ ,  $\eta_{eg_3}$  are the efficiency of the listed electric generators.

The specific fuel consumption at the CGSTU's power plant

$$C_{Ne} = \frac{G_{fh} + G_{fh_2}}{N_{eGTE} + N_{eST} + N_{eSIGT}} \quad (13)$$

where  $G_{fh}$  and  $G_{fh_2}$  are the hourly fuel consumption of the base GTE and the SIGT, respectively.

The efficiency of the CGSTU's power plant

$$\eta_{eCGSTU} = \frac{3600}{C_{Ne} \cdot H_U} \quad (14)$$

### 3. OPTIMIZATION OF THE PARAMETERS OF THE COMBINED GAS-STEAM TURBINE UNIT OF A HYBRID CYCLE

Figure 2 shows the dependences of the efficiency of the combined CGSTU of a hybrid cycle on the total compressor pressure ratio  $\pi_{c\Sigma}$  in the SIGT and the exhauster compression ratio  $\pi_{ex}$ . The results were obtained for the case of injection of the entire amount of steam generated by the HRSG located behind the base GTE into the SIGT at the temperature of the gas-steam mixture at the turbine inlet  $T_3 = 1500$  K and the air excess coefficient in the combustion chamber  $\alpha_0 = 1.5$ .

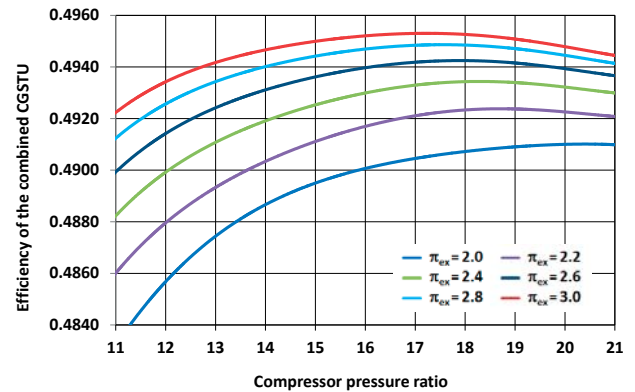


Fig. 2. Dependences of the efficiency of the combined CGSTU of a hybrid cycle for a thermal power station on the compressor and exhauster pressure ratios.

Analysis of the data shows the possibility of achieving the efficiency of the combined CGSTU at the level of 49.1–49.5% with the optimal compressor pressure ratio of 16–20 in the SIGT and varying the exhauster pressure ratio in the range from 2.0 to 3.0.

Figure 3 shows the dependences of the electric power of the combined CGSTU of a hybrid cycle on the compressor pressure ratio in the SIGT and the exhauster pressure ratio for the same initial conditions.

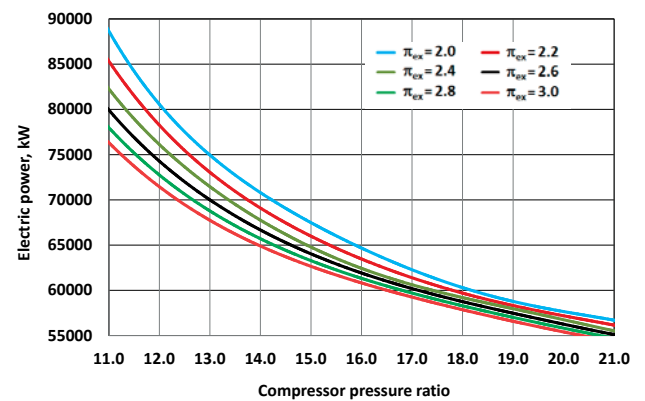


Fig. 3. Dependences of the electric power of the combined CGSTU of a hybrid cycle on the compressor and exhauster pressure ratios.

The analysis shows the possibility of achieving the electric power of the power plant at the level of 55–65 MW with the optimal compressor pressure ratio of 16–20 in the SIGT and a change in the exhauster pressure ratio in the range from 2.0 to 3.0.



The investigation of the influence of the air excess coefficient  $\alpha_0$  in the SIGT combustion chamber on the efficiency indicators of the CGSTU (Fig. 4) shows that with an increase in the value of this parameter from 1.5 to 2.0, the efficiency of the installation increases from 49.4 to 50.6%, and the optimal SIGT compressor pressure ratio  $\pi_{c\Sigma}$  decreases from 17.5 to 11.5. The results presented were obtained at the temperature of the gas-steam mixture at the turbine inlet  $T_3 = 1500$  K and the exhauster pressure ratio  $\pi_{ex} = 2.6$ .

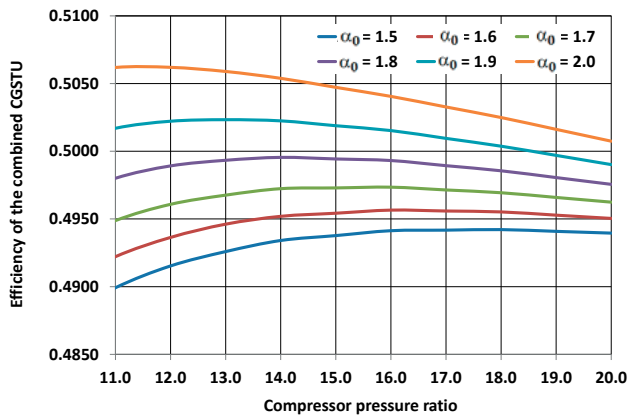


Fig. 4. Dependences of the efficiency of the CGSTU of a hybrid cycle on the compressor pressure ratio and the air excess coefficient in the SIGT.

The graphs of the dependences of the electric power of the combined CGSTU of a hybrid cycle on the SIGT compressor pressure ratio  $\pi_{c\Sigma}$  and the air excess coefficient  $\alpha_0$  in the combustion chamber for the same initial conditions are shown in Fig. 5.

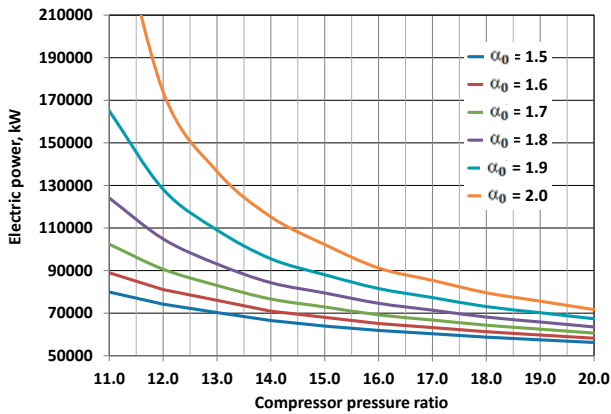


Fig. 5. Dependences of the electric power of the combined CGSTU of a hybrid cycle on the SIGT compressor pressure ratio and the air excess coefficient in the combustion chamber.

The analysis of the dependencies shows the possibility of achieving the electric power of the power plant at the level of 60–210 MW at the values of the optimal SIGT compressor ratios from 17.5 to 11.5, respectively.

The combined CGSTU of a hybrid cycle for a thermal power station is supposed to be used in the power range of 50–80 MW. In this regard, the possibility of the partial supply of steam generated by the HRSG behind the UGT25000 gas turbine

engine to the SIGT combustion chamber with constant electric generator power, driven from the steam turbine of the base GTE HRC, is considered. For the subsequent analysis, let us introduce the parameter of the partial steam supply  $X$ , which is the ratio of the mass flow rate of steam, which is injected into the SIGT combustion chamber, to the total steam flow rate generated by the HRC of the base gas turbine engine.

Figure 6 shows the dependences of the efficiency of the combined CGSTU of a hybrid cycle on the SIGT compressor pressure ratio and the amount of steam injected into the SIGT combustion chamber from the HRSG located behind the base engine, and Fig. 7 shows the dependences of the electric power of a thermal power station on the same parameters. The results were obtained for the temperature of the gas-steam mixture at the SIGT turbine inlet  $T_3 = 1500$  K, the air excess coefficient in the combustion chamber  $\alpha_0 = 1.8$ , and the exhauster pressure ratio  $\pi_{ex} = 2.6$ .

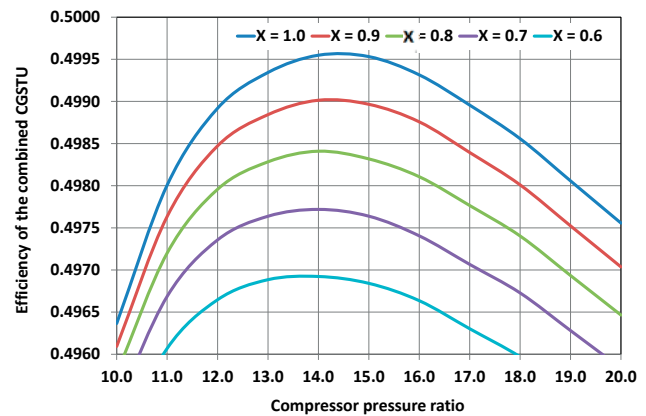


Fig. 6. Dependences of the efficiency of the combined CGSTU of a hybrid cycle on the SIGT compressor pressure ratio and the parameter of the partial steam supply.

Analysis of the graphical dependencies shows a decrease in the efficiency of the CGSTU by 0.11–0.16% and a decrease in the power of the power plant by 6.3–7.2% for every 10% decrease in the mass quantity of injected steam in the considered range of its flow rates. Thus, for example, by injecting 60% of steam from its total amount, it is possible to reduce the power of the installation from 84.3 to 64.3 MW (Fig. 7).

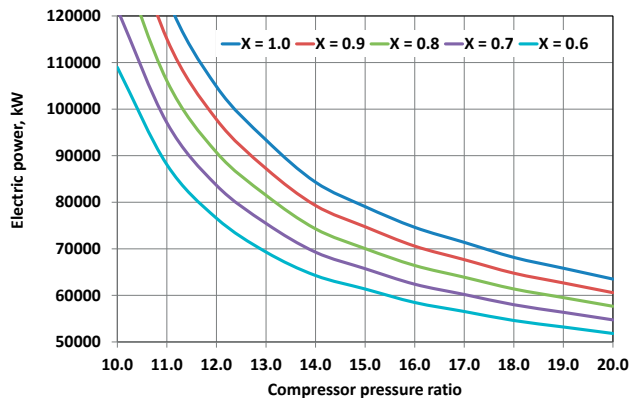


Fig. 7. Dependences of the electric power of the CGSTU on the SIGT compressor pressure ratio and the parameter of the partial steam supply.

Note that a decrease in the amount of steam supplied to the SIGT combustion chamber has a very weak effect on the value of the optimal SIGT compressor pressure ratio. Thus, the optimal SIGT compressor pressure ratio varies from 14.5 to 14.0 with a decrease in the steam supply by 60%.

To substantiate the choice of the temperature of the gas-steam mixture at the SIGT turbine inlet, the influence of this parameter (in the range of 1500-1560 K) on the efficiency indicators of the investigated CGSTU is considered. As follows from the graphical dependencies in Fig. 8, with an increase in the value of this parameter, the CGSTU efficiency increases from 49.7 to 51.15%, and the optimum compressor pressure ratio  $\pi_{c\zeta}$  is reduced from 14.2 to 9.5. The above results were obtained with the air excess coefficient in the SIGT combustion chamber  $\alpha_0 = 1.8$ , the exhauster pressure ratio  $\pi_{ex} = 2.6$ , and with injection to the combustion chamber of 60% of the steam generated by the HRSG behind the base engine.

The influence of the temperature of the gas-steam mixture at the SIGT turbine inlet in the range of 1500-1560 K on the electric power of the combined CGSTU of a hybrid cycle can be estimated from the data in Fig. 9 obtained for the same initial conditions. An increase in the power of the power plant of 4-7% is observed for each increase in the temperature  $T_3$  by 10 degrees.

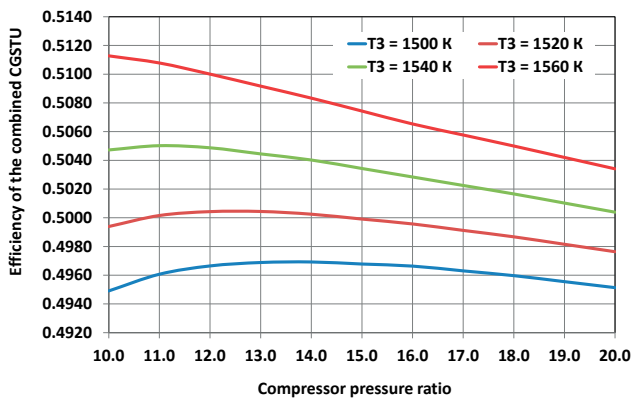


Fig. 8. Dependences of the efficiency of the combined CGSTU of a hybrid cycle on the SIGT compressor pressure ratio and the temperature of the gas-steam mixture at the turbine inlet.

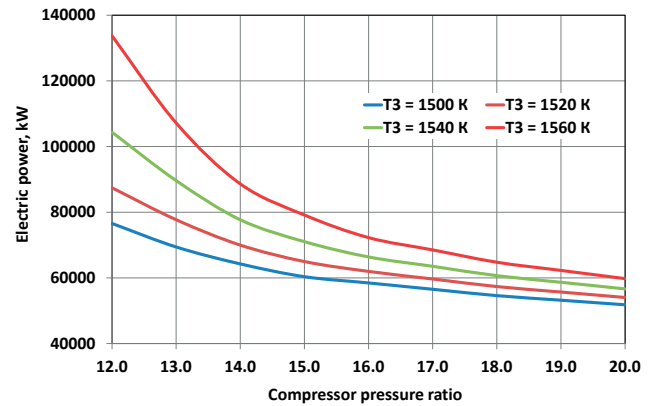


Fig. 9. Dependence of the electric power of the combined CGSTU of a hybrid cycle on the SIGT compressor pressure ratio and the temperature of the gas-steam mixture at the turbine inlet.

The analysis of the capabilities of the combined CGSTU of a hybrid cycle when using the UGT25000 gas turbine engine as the base engine makes it possible to recommend the optimal (taking into consideration the accepted technical limitations) combinations of heat recovery circuits design parameters. These parameters (Table 1) are the pressure  $P_{HRSG}$  and temperature of the superheated steam  $T_{ss}$ , the parameter of the partial steam supply  $X$  into the SIGT combustion chamber, as well as the parameters of the steam-injected gas turbine and the exhauster, depending on the estimated electric capacity  $N_{elCGSTU}$  of the power plant. The effective power of the steam-injected gas turbine  $N_{eSIGT}$  and steam turbine  $N_{eST}$  the air flow rate  $G_{cSIGT}$  through the SIGT, and the efficiency of the installation  $\eta_e$  depending on the optimized parameters, are given in Table 1.

Figure 10 shows the dependences of the specific fuel consumption during the operation of the basic GTE, the basic GTE together with a steam turbine, and during the operation of the combined gas-steam turbine unit with a hybrid cycle for an 80 MW thermal power station, depending on the load. Calculations show that power up to 14 MW is provided by the operation of only the basic GTE UGT25000 (simple thermodynamic cycle). To achieve a power of 14-33 MW, it is sufficient to operate a gas turbine engine and a steam turbine, providing a specific fuel consumption of 0.156 kg/(kW·h) at a load of 33 MW (binary steam-gas cycle). Higher powers of 33-80 MW are covered by the joint work of the entire energy complex of the CGSTU, including a steam-injected gas turbine. In this case, the specific fuel consumption is reduced to 0.146 kg/(kW·h) at a load of 80 MW.

Tab. 1. Parameters of the CGSTU of a hybrid cycle.

$N_{elCGSTU}$ , MW	$N_{eSIGT}$ , MW	$N_{eST}$ , MW	$G_{cSIGT}$ , kg/s	$\eta_e$ , %	$\pi_{c\zeta}$	$T_3$ , K	$\alpha_0$	$\pi_{ex}$	$P_{HRSG}$ , MPa	$T_{ss}$ , K	$X$
50	20.42	4.80	18.00	49.60	14.5	1500	1.66	2.8	1.56	715	0.40
60	31.45	3.99	30.48	49.91	14.0	1510	1.72	2.6	1.51	710	0.50
70	41.58	3.98	43.18	50.43	13.85	1528	1.78	2.6	1.49	706	0.50
80	51.76	3.97	55.67	50.72	13.35	1536	1.80	2.6	1.44	704	0.50
90	62.54	3.96	69.32	50.88	12.85	1537	1.82	2.6	1.385	699	0.50
100	72.44	3.95	82.26	50.97	12.5	1535	1.84	2.6	1.35	696	0.50

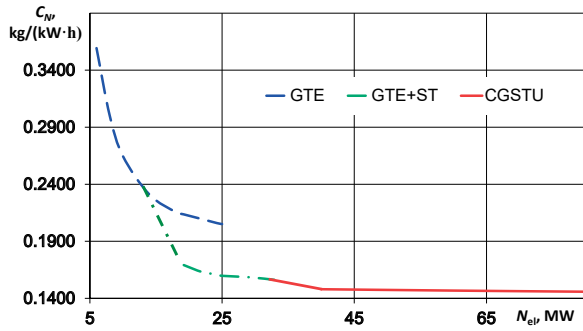


Fig. 10. Dependences of specific fuel consumption on the CGSTU power.

#### 4. ECOLOGICAL CHARACTERISTICS OF THE COMBUSTION CHAMBER OF A STEAM-INJECTED GAS TURBINE

One of the important issues that determine the applicability of heat engines for work in a thermal power station is their environmental performance. As mentioned above, the injection of ecological steam into the primary zone of the combustion chamber is an effective method for reducing nitrogen oxide emissions. To analyze the emission characteristics of a 51.76 MW steam-injected gas turbine as part of an energy system with a total electric power of 80 MW (Table 1), the corresponding three-dimensional calculations of the working process of the gas turbine combustion chamber with the injection of ecological and power steam were carried out.

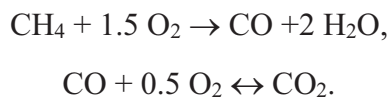
The modeling of physical and chemical processes in the combustion chamber of a steam-injected gas turbine is based on solutions of the differential equations of mass, impulse, and energy conservation for the multi-component, turbulent, chemically reacting system [15-17].

The source of chemical species  $m$  due to reaction  $R_m$  is computed as the sum of the reaction sources over the  $k$  reactions

$$R_m = \sum_k R_{mk}, \quad (15)$$

where  $R_{mk}$  is the rate of formation (destruction) of species  $m$  during reaction  $k$ .

Combustion in the gaseous phase is modeled as simple two-step chemical reactions:



The reaction rate is calculated considering the Arrhenius, Magnussen, and Hjertager models [18]:

$$R_{mk} = v_{mk} M_m T^{\beta_k} A_k \prod_j [C_j]^{v_{jk}^l} \exp(-E_k/RT), \quad R_{mk} = A \rho \frac{\varepsilon}{k} \frac{X_m}{v_{mk}} \quad (16)$$

where  $v_{mk}$  is the stoichiometric coefficient,  $M_m$  is the molecular weight of species  $m$ ,  $\beta_k$  is the temperature exponent,  $A_k$  is the pre-exponential factor,  $C_j$  is the molar concentration of each species  $j$ ,  $v_{jk}^l$  is the concentration exponent,  $E_k$  is the activation energy,  $R$  is the gas constant,  $A$  is the empirical constant;  $\rho$  is the mass density,  $k$  is the turbulent kinetic energy,  $\varepsilon$  is the turbulent dissipation rate, and  $X_m$  is the mass fraction of chemical species  $m$ .

The reaction rate is taken to be the smaller of these two expressions. This chemistry-turbulence approach is used because there are regions within the steam-injected combustion chamber where the turbulent mixing rate is faster than the chemical kinetics.

To predict the emission of nitrogen oxide NO, the mass transfer equation, which includes convection, diffusion, and formation/decomposition of NO, is used [19]:

$$\nabla \cdot (\rho \vec{v} Y_{\text{NO}}) = \nabla \cdot (\rho D \nabla Y_{\text{NO}}) + S_{\text{NO}} \quad (17)$$

where  $Y_{\text{NO}}$  is the NO mass concentration,  $D$  is the diffusion coefficient,  $\vec{v}$  is the velocity vector, and  $S_{\text{NO}}$  is the source term depending on the  $\text{NO}_x$  formation mechanism.

Note that such a model was previously used to predict the characteristics of the combustion chamber of a 16 MW steam-injected gas turbine. Calculated and experimental distributions of the emission of toxic components (nitrogen oxides and carbon monoxide), as well as temperatures, confirmed the adequacy of the mathematical model [15, 16].

The combustion chamber of the "Aquarius" type gas turbine engine was chosen for investigation (Fig. 11). In this combustion chamber, the injection of the ecological and power steam is realized. The combustion chamber has a cannular design with twenty flame tubes. The main feature of its design is the injection of ecological steam into the primary combustion zone and power steam into the mixing zone, which allows the specific engine power to be increased and enhances the ecological parameters.

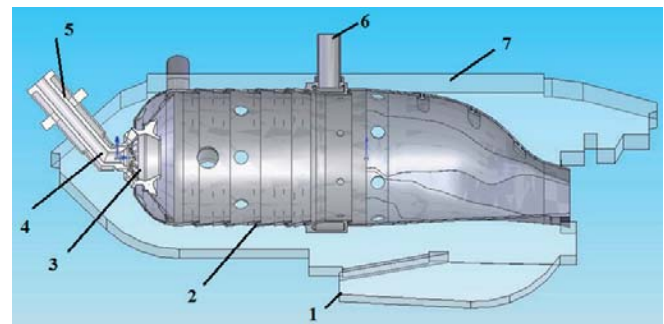


Fig. 11. The scheme of the investigated combustion chamber: 1 – air after compressor; 2 – flame tube; 3 – swirler; 4 – nozzle; 5 – ecological steam injection; 6 – power steam injection; 7 – casing.



In the calculations, the amount of ecological steam injected into the primary zone was 30% of the total amount of steam supplied to the combustion chamber.

Figure 12 shows the contours of the temperature and mass fractions of  $\text{CH}_4$ ,  $\text{CO}$ , and  $\text{H}_2\text{O}$  inside the combustion chamber. It can be seen that active fuel burnout begins not near the nozzle, but at some distance from the fuel injection sections. This is due to some overcooling of the primary chamber's zone due to the injection of ecological steam and an increase in the velocity of the fuel-air-steam mixture in it. Despite this, the fuel burnout is practically completed

before the cross-section of the injection of radial air jets into the flame tube. These radial jets transform the burning fuel flame in a certain way and intensify the mixing of the components. Directly behind the vane swirler, a system of recirculation flows is formed, which stabilizes the position of the flame front and, despite the cooling effect of the ecological steam, ensures the ignition of fresh portions of fuel. Note that in several operation modes, especially with an increase in the flow rate of ecological steam, it may be necessary to use additional stabilizers, for example, plasma igniters and intensifiers [20, 21].

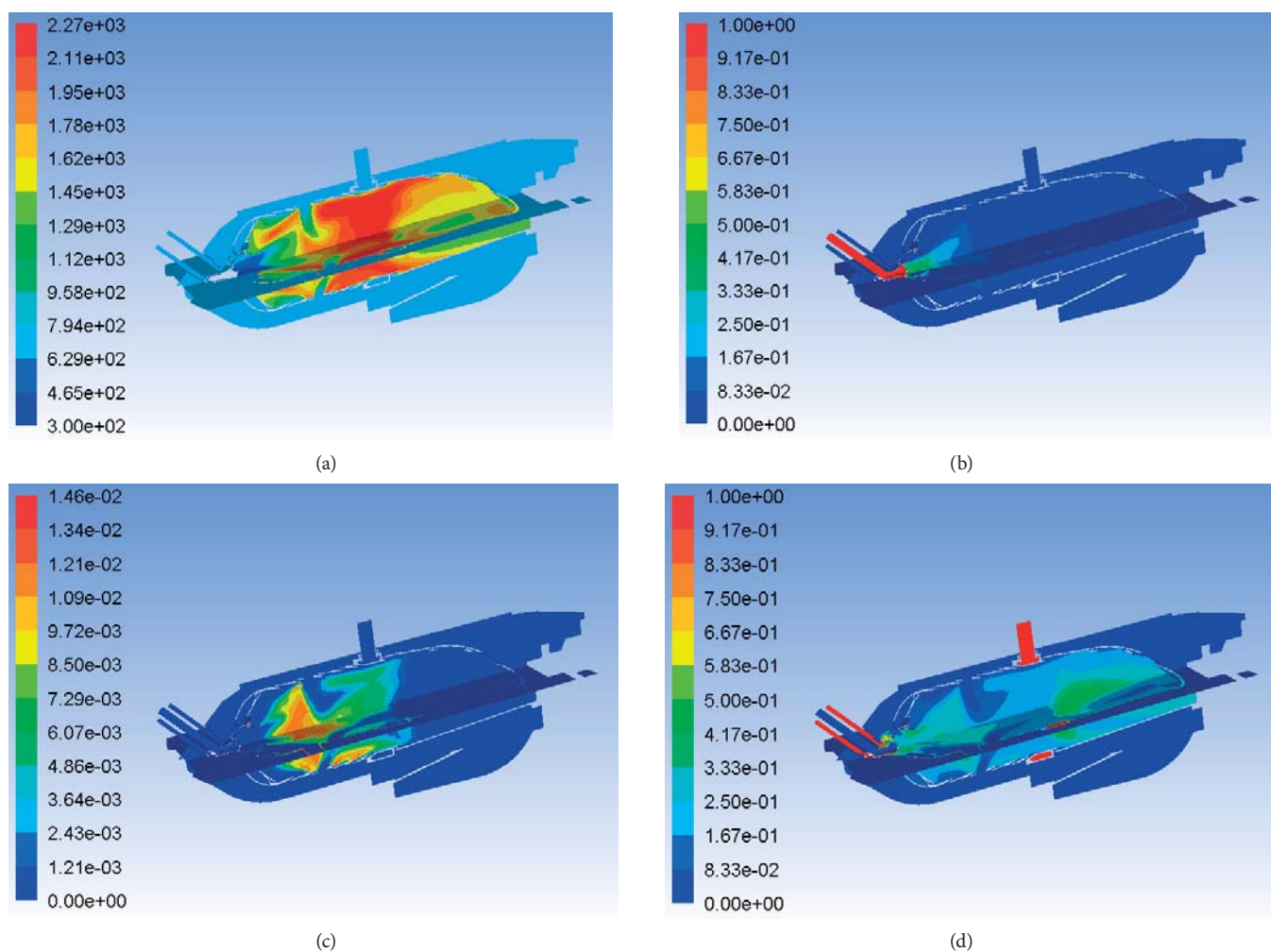
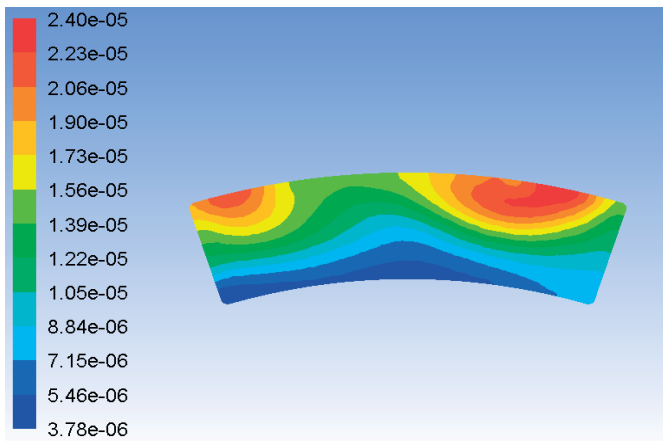


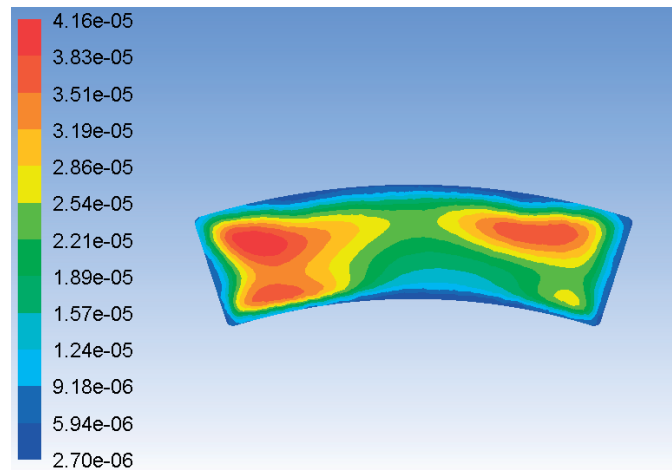
Fig. 12. Contours of temperature, K (a), and mass fractions of  $\text{CH}_4$  (b),  $\text{CO}$  (c),  $\text{H}_2\text{O}$  (d) inside the combustion chamber.

Figure 13 shows the contours of the mole fractions of the main pollutants: nitrogen oxide and carbon monoxide in the outlet section of the flame tube. The uneven distribution of these components over the outlet section is visible, which is explained by the rather high uneven distribution of the power steam in the dilution zone of the combustion chamber. This requires further optimization of the power steam feeding design.

Despite the somewhat prolonged process of carbon monoxide burnout, its calculated emission at the combustion chamber outlet is 22.4 ppm. At the same time, the calculated emission of nitrogen oxide  $\text{NO}$  is equal to 12.3 ppm, which satisfies the modern requirements for gas turbine engines.



(a)



(b)

Fig. 13. Contours of mole fractions of NO (a) and CO (b) at the combustion chamber outlet.

## CONCLUSIONS

The thermal diagram of the combined gas-steam turbine unit of a hybrid thermodynamic cycle for a thermal power station, developed based on a serial gas turbine engine, is considered. The thermal diagram also includes a steam-injected gas turbine operating with overexpansion and a steam turbine heat recovery circuit for a serial gas turbine engine. Analysis of the calculation results revealed the following.

1. The possibility of creating a combined gas-steam turbine unit based on a serial gas turbine engine with a capacity of 26,700 kW and efficiency of 36.3% for a thermal power station with capacity up to 100 MW and efficiency of 49.6-51% using a hybrid thermodynamic cycle is shown.

2. The design optimal parameters of the steam-injected gas turbine have been substantiated and, for a thermal power station capacity range from 50 to 100 MW, should have a capacity from 20.4 to 72.4 MW, respectively.

3. It is proposed for the temperature level of the working fluid behind the combustion chamber of 1500-1400 K to accept the total compressor pressure ratio of 12.5-14.5 in the steam-injected gas turbine at the exhaust compression ratio of 2.6-2.8.

4. The rational values of the air excess coefficient in the range of 1.66-1.84 for the combustion chamber of the steam-injected gas turbine were determined when injecting 40-50% of steam, which is generated by the heat recovery circuit of the base gas turbine engine.

5. The three-dimensional calculations of the working process in the combustion chamber of a 51.76 MW steam-injected gas turbine confirmed the feasibility of dividing the injected steam into ecological and energy steam. The first determines the required emission characteristics of the combustion chamber, and the second leads to an increase in the specific power of the gas-steam turbine plant.

## REFERENCES

1. Kehlhofer R. Combined-cycle gas and steam turbine power plants. Penn Well Publishing Co. 1997;388.
2. Carcasci C., Pacifici B., Winchler L., Cosi L., Ferraro R. Thermo-economic Analysis of a One-Pressure Level Heat Recovery Steam Generator Considering Real Steam Turbine Cost. *Energy Procedia* 2015; 82:591-598.
3. Nirbito W., Arif Budiyo M., Muliadi R. Performance Analysis of Combined Cycle with Air Breathing Derivative Gas Turbine, Heat Recovery Steam Generator, and Steam Turbine as LNG Tanker Main Engine Propulsion System. *J. Mar. Sci. Eng.* 2020; 8(726):1-15.
4. Matveev I.B., Serbin S.I., Washchilenko V.N. Plasma-assisted treatment of sewage sludge. *IEEE Trans. Plasma Sci.* 2016; 44(12):3023-3027.
5. Cheng D.Y., Nelson, A.L.C. The chronological development of the Cheng cycle steam injected gas turbine during the past 25 years. *Proceeding of ASME Turbo Expo 2002*, Amsterdam, GT-2002-30119. 2002;1-8.
6. Bondin Y.N., Krivutsa V.A., Movchan S.N., Romanov V.I., Kolomeev V.N., Shevtsov A.P. Operation experience of a gas turbine unit GPU-16K with steam injection. *Gas Turbine Technologies* 2004; 5:18-20 (in Russian).
7. Movchan S.N., Romanov V.V., Chobenko V.N., Shevtsov A.P. Contact Steam-and-Gas Turbine Units of the "AQUARIUS" Type: The Present Status and Future Prospects. *Conference: ASME Turbo Expo 2009: Power for Land, Sea, and Air*. 2009;1-7.

8. Romanovsky G.F., Washchilenko N.V., Serbin S.I. Theoretical bases of designing ship gas turbine units. Ukrainian State Maritime Technical University. 2003 (in Ukrainian).
9. Offshore Magazine. Leadon FPSO delivered on time, complete, within budget. 2002. <https://www.offshore-mag.com/production/article/16759844/leadon-fps-delivered-on-time-complete-within-budget>.
10. Cherednichenko O., Serbin S., Dzida M. Application of thermo-chemical technologies for conversion of associated gas in diesel-gas turbine installations for oil and gas floating units. *Polish Maritime Research* 2019; 3(103):181-187.
11. Ocyan. FPSO Cidade de Itajaí. 2017. [https://api.ocyancsa.com/sites/default/files/2018-09/cidade\\_do\\_itajai\\_0.pdf](https://api.ocyancsa.com/sites/default/files/2018-09/cidade_do_itajai_0.pdf).
12. Offshore Technology. Triton Oil Field, North Sea Central. 2018. <https://www.offshore-technology.com/projects/triton/>.
13. Gas Turbine Engine UGT25000, <https://zmturbines.com/en/serial-production/engines/ugt-25000/>.
14. Gas Turbine World. 2004-05 GTW Handbook, Pequot Publishing Inc., 2006.
15. Serbin S.I., Kozlovskiy A.V., Burunsuz K.S. Investigations of non-stationary processes in low emissive gas turbine combustor with plasma assistance. *IEEE Trans. Plasma Sci.* 2016; 44(12):2960-2964.
16. Matveev I.B., Serbin S.I., Vilkul V.V., Goncharova N.A. Synthesis Gas Afterburner Based on an Injector Type Plasma-Assisted Combustion System. *IEEE Trans. Plasma Sci.* 2015; 43(12):3974-3978.
17. Matveev I., Serbin S., Mostipanen A. Numerical optimization of the "Tornado" combustor aerodynamic parameters. *Collection of Technical Papers. 45th AIAA Aerospace Sciences Meeting*, Reno, Nevada, AIAA 2007-391. 2007; 7:4744-4755.
18. Magnussen B.F., Hjertager B.H. On mathematical models of turbulent combustion with special emphasis on soot formation and combustion. *16th Int. Symp. on Combustion*. The Combustion Institute. 1976; 16(1):719-729.
19. Launder B.E., Spalding D.B. *Lectures in Mathematical Models of Turbulence*. London: Academic Press; 1972.
20. Serbin S.I., Matveev I.B. Theoretical and experimental investigations of the plasma-assisted combustion and reformation system. *IEEE Trans. Plasma Sci.* 2010; 38(12):3306-3312.
21. Serbin S.I., Matveev I.B., Goncharova N.A. Plasma assisted reforming of natural gas for GTL. Part I. *IEEE Trans. Plasma Sci.* 2014; 42(12):3896-3900.

## CONTACT WITH THE AUTHORS

**Serhiy Serbin**

*serbin1958@gmail.com*

Admiral Makarov National University of Shipbuilding,  
Geroes of Ukraine, 54025 Mikolayiv,

**UKRAINE**

**Nikolay Washchilenko**

*e-mail: nnuy5te@gmail.com*

Admiral Makarov National University of Shipbuilding,  
Geroes of Ukraine, 54025 Mikolayiv,

**UKRAINE**

**Marek Dzida**

*e-mail: dzida@pg.edu.pl*

Gdańsk University of Technology,  
Gabriela Narutowicza Street, 80-233 Gdańsk,

**POLAND**

**Jerzy Kowalski**

*e-mail: jerzy.kowalski@pg.edu.pl*

Gdańsk University of Technology,  
Gabriela Narutowicza Street, 80-233 Gdańsk,

**POLAND**